UNIVERSITÀ DEGLI STUDI FIRENZE

FLORE
Repository istituzionale dell'Università degli Studi di Firenze

UV Transient Brightenings Associated with a Coronal Mass Ejection

Questa è la Versione finale referata (Post print/Accepted manuscript) della seguente pubblicazione:

Original Citation:

UV Transient Brightenings Associated with a Coronal Mass Ejection / G. Schettino;G. Poletto;M. Romoli. - In: THE ASTROPHYSICAL JOURNAL LETTERS. - ISSN 2041-8205. - STAMPA. - 697:(2009), pp. L72-L76. [10.1088/0004-637X/697/1/L72]

Availability:

This version is available at: 2158/383057 since:

Published version:

DOI: 10.1088/0004-637X/697/1/L72

Terms of use:

Open Access

La pubblicazione è resa disponibile sotto le norme e i termini della licenza di deposito, secondo quanto stabilito dalla Policy per l'accesso aperto dell'Università degli Studi di Firenze (https://www.sba.unifi.it/upload/policy-oa-2016-1.pdf)

Publisher copyright claim:

(Article begins on next page)

12 October 2024

The Astrophysical Journal, 697:L72–L76, 2009 May 20 doi:10.1088/0004-637X/697/1/L72
© 2009. The American Astronomical Society. All rights reserved. Printed in the U.S.A.

UV TRANSIENT BRIGHTENINGS ASSOCIATED WITH A CORONAL MASS EJECTION

G. Schettino[1], G. Poletto[2], and M. Romoli[1]
[1] Dipartimento di Astronomia e Scienza dello Spazio, Università di Firenze, Largo E. Fermi 2, 50125 Florence, Italy; giulia@arcetri.astro.it
[2] INAF-Osservatorio Astrofisico di Arcetri, Largo E. Fermi 5, 50125 Florence, Italy
Received 2009 February 27; accepted 2009 April 20; published 2009 May 1

ABSTRACT

In this paper, we analyze transient UV brightenings in spectra acquired by *SOHO*/UltraViolet Coronagraph Spectrometer (UVCS) on 2003 June 2 in association with a coronal mass ejection (CME) that occurred at the West limb of the Sun at 08:54 UT. Brightenings have been observed in lines from cool (C III, O VI), intermediate (Si VIII, Si XII), and high ([Fe XVIII]) temperature ions over about 7 hr from the CME. Brightenings in cool lines are interpreted in terms of mini-ejections that appear at the time of, and after, the passage of the CME front through the UVCS slit. We give here their temperature and density and we point out that, assuming a spherical shape, a few of these mini-CMEs can provide a mass comparable to that quoted for typical CMEs. Hot lines, like the [Fe XVIII] line at 974.9 Å which shows up in the CME associated current sheet (CS), undergo transient brightness as well, but hot lines brightenings are more difficult to interpret. We propose here a scenario where they are signatures of the passage through the UVCS slit of plasmoids similar to those observed in the filamentary CS of the magnetotail that form as a consequence of the tearing-mode instability or of a time-dependent Petschek-type reconnection.

Key words: Sun: coronal mass ejections (CMEs) – Sun: UV radiation

1. INTRODUCTION

Coronal mass ejections (CMEs) are sudden expulsions of coronal plasma from the solar surface into the interplanetary space, produced by a loss of equilibrium in the magnetic configuration. There is a general consensus about the role played by magnetic reconnection in the evolution of a CME. First ideas that, as a result of the loss of equilibrium in the magnetic system, a thin current sheet (CS) forms between the top of the flare loops and the CME bubble can be found in the CSHKP models (Carmichael 1964; Sturrock 1966; Hirayama 1974; Kopp & Pneuman 1976) and have been developed in recent models like, e.g., the "catastrophe model" by Lin & Forbes (2000). Observational evidence of the formation of a CS after the CME eruption has been found in many events (e.g., Ciaravella et al. 2002; Ko et al. 2003; Raymond et al. 2003; Lin et al. 2005; Bemporad et al. 2006; Ciaravella & Raymond 2008).

At the time of the ejection of a CME, LASCO coronagraphs often observed transient white light enhancements in the coronal brightness, usually referred to as blobs. These blobs move outward along the CS and are considered as one of the most significant evidences of reconnection in CSs (see, e.g., Lin et al. 2008). Usually they are interpreted (see, e.g., Lin et al. 2007) in terms of magnetic islands produced as the result of the tearing-mode instability (Furth et al. 1963), or invoking time-dependent Petschek-type reconnection (see, e.g., Priest & Forbes 2000). These interpretations establish a link between solar and magnetospheric reconnection: blobs should be identified with plasmoids, which are known to form in the terrestrial magnetosphere (Hones 1985) and which have been first discovered in the ISEE data by Hones et al. (1984) and Slavin et al. (1984), and have been described in terms of magnetic islands in the CS. Recently, observations from the CLUSTER spacecraft confirmed this magnetic island structure and led to an interpretation in terms of multiple X-line reconnection (e.g., Slavin et al. 2003, 2005; Eastwood et al. 2005).

Blobs associated with CMEs have been studied in white light by Ko et al. (2003) and Lin et al. (2005). From LASCO observations Ko et al. (2003) recognized about 10 transient features in the CS associated with a CME that occurred on 2002 January 8 and dubbed them as "plasma blobs." They inferred for one of these blobs a projected dimension of 340″ and an electron density $N_e = 3.4 \times 10^6$ cm^{-3} at $4.4 R_\odot$, while for another blob they obtained a value $N_e = 4.0 \times 10^6$ cm^{-3} at $3.0 R_\odot$. Numerical simulations of formation of outflowing blobs in a CS produced after a CME have been performed by several authors (e.g., Riley et al. 2007; Bárta et al. 2008).

Recently, transient brightenings associated with CMEs have been observed by Ciaravella & Raymond (2008) with the UltraViolet Coronagraph Spectrometer (UVCS) at 1.7 $R_\odot$, that is, at a lower heliocentric distance than blobs observed by LASCO. They recognized as blobs some cold and narrow (126″) transient, brightening in O VI, C III, and other low temperature ions lines, which crossed the UVCS slit from 1 to 15 hr after the CME ejection. From EUV Imaging Telescope (EIT) and *Transition Region and Coronal Explorer* (*TRACE*) images Ciaravella and Raymond concluded that the blobs originated from the same source in the active region underlying the CME and proposed that these features were produced by minor reconnection events associated with the rearrangement of the magnetic configuration after the CME eruption. They also identified in LASCO C2 images many blobs moving outward along the CS structure or adjacent to the CS.

Nevertheless, despite the results described above, not much is known about the physical condition of plasma blobs associated with CMEs. In this work, we analyze transient brightenings from cold and hot temperature ions, observed by UVCS at $1.7 R_\odot$ in association with a CME that occurred on 2003 June 2. We give, for the first time, their electron temperatures and densities and, by assuming a spherical shape, we also estimate the mass of the cool temperature blobs and their contribution to the total CME mass. We further discuss transient brightenings in the [Fe XVIII] line, whose behavior suggests an interpretation in terms of plasmoids in a filamentary CS structure.

2. THE UVCS OBSERVATIONS

The LASCO CME catalog shows that on 2003 June 2 a partial-halo CME occurred at 08:54 UT at a position angle, measured

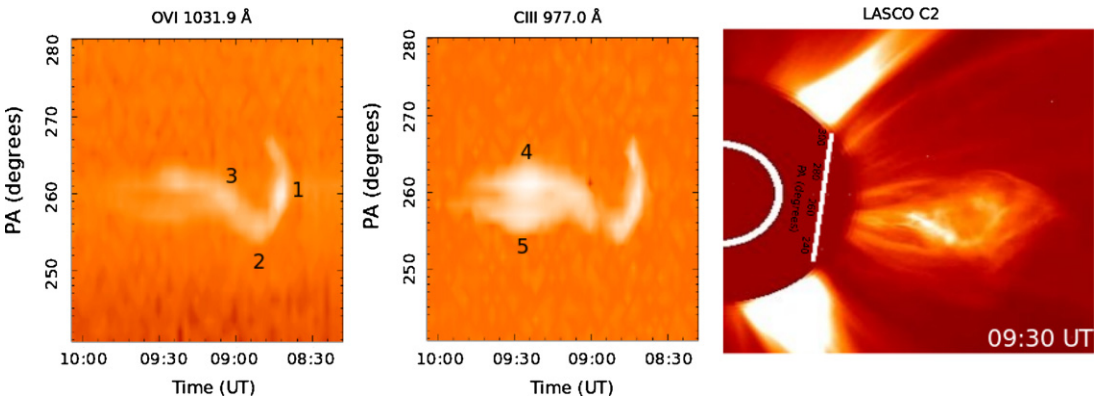

Figure 1. Left and middle: O VI 1031.9 Å and C III 977.0 Å intensity maps. On the *x*-axis we give the time of observation, on the *y*-axis the position along the UVCS slit, converted into position angles (P.A.). Right: LASCO C2 image at 09:30 UT.

counterclockwise from the North Pole, P.A. = 261°, moving at a projected speed of 980 km s^{-1}. On that day UVCS acquired data from 06:08 UT to 15:58 UT with the slit centered above the west limb at a position angle P.A. = 263° at an heliocentric height of $1.7R_{\odot}$. Data were acquired with an exposure time of 2 minutes and with a spatial binning of 6 pixels (42″ in spatial resolution). The slit width was 98 μm. Five spectral ranges were selected on the detector (1023.97–1043.23, 1005.00–1013.14, 998.05–1002.02, 967.17–981.07, 943.38–966.32 Å) with a 2 pixel spectral binning (0.1986 Å) in the first four panels and a 3 pixel binning (0.2979 Å) in the fifth. These spectral intervals include lines from ions with both high and low temperatures of the line formation: the strongest lines are O VI 1031.9–1037.6 Å ($\log T_{\max} = 5.5$), H I Lyβ ($\log T_{\max} = 4.2$) and, for the second order, Si XII 499.4 Å ($\log T_{\max} = 6.3$), but [Fe XVIII] 974.9 Å ($\log T_{\max} = 6.8$) and C III 977.0 Å ($\log T_{\max} = 4.9$) lines are also included. This latter line can be used to correct the stray-light contamination, while [Fe XVIII] line is used to identify CSs. Data calibration has been performed using the standard routines of the Data Analysis Software (DAS40). After the calibration, we computed the intensity of each line in the data set by integrating over the line profile, subtracting the adjacent background and correcting for stray light.

Looking at UVCS spectra, an enhancement in O VI, C III, H I Lyβ, and Lyγ line intensities, that starts at 08:39 UT, led us to interpret it as an evidence that the CME front reached the UVCS slit at $1.7R_{\odot}$. The maps of the intensity profiles of O VI 1031.9 Å and C III 977.0 Å lines along the portion of the UVCS slit crossed by the front are shown in Figure 1, together with a LASCO C2 image of the event. In both maps we give the time of observation on the *x*-axis and the position along the UVCS slit on the *y*-axis; superposed onto the LASCO image, taken at 09:30 UT, we give the position of the UVCS slit projected on the plane of the sky.

A comparison between the LASCO C2 image (Figure 1, right panel) with the left panels, reveals how the structure of the CME front, and the "stem" under the CME bubble, usually identified with the CME-associated CS (Vršnak et al. 2009), appear in UVCS data. We point out that the CME bubble looks inhomogeneous both in the UVCS intensity maps and in the LASCO image: in O VI and C III maps we identified five intensity enhancements within localized structures, hereafter referred to as plasma blobs. We classified each blob with a number from 1 to 5, as shown in Figure 1. The lines identified in each blob, their P.A.s, the time of the transit through the UVCS slit and their Doppler shift are listed in Table 1.

Table 1
Blobs Associated with the 2003 June 2, 08:54 UT CME

Blob	Observed Lines	P.A. (deg)	Transit Time (UT)	Doppler Shift (Å)
1	Si VIII, Si XII, O VI	260.0	08:42–08:46	-0.7 ± 0.1
2	C III, O VI	254.8	08:51–08:57	-1.0 ± 0.1
3	C III, O VI, Lyβ	257.7	09:01–09:10	···
4	C III, O VI, Lyβ, Lyγ	260.7	09:21–09:29	···
5	C III	255.6	09:21–09:29	···

All these blobs are bright in O VI doublet lines, but the first shows the presence of emission from "intermediate" temperature ions, Si VIII ($\log T_{\max} = 5.9$) and Si XII ($\log T_{\max} = 6.3$), while the others are detectable only from the emission of low temperature ions. Lines in the CME front turned out to have an average blueshift of about −0.6 Å, decreasing from a maximum value of −1.2 Å at 08:39 UT to zero after 09:01 UT. Hence, we conclude that blobs 1 and 3 seem to be part of the CME bubble structure, while blob 2 is a feature adjacent to the front. Blobs 4 and 5 appear after the passage of the CME front, in the position where we detected, from 09:40 UT onward, the presence of a CS. We now turn to the analysis of UVCS "hot" lines. From 09:40 UT to the end of the data set (15:58 UT) emission from [Fe XVIII] 974.9 Å line shows up, together with an enhancement in Si XII 499.4 Å line intensity, over a latitude interval P.A. = 253°–266°. As we mentioned, [Fe XVIII] emission is usually interpreted as a signature of CSs. For a better identification of its behavior and to improve the line statistics, we grouped the UVCS data from 09:40 UT to the end of the data set in nine intervals summing over an increasing number of exposures (9:40–10:10, 10:10–10:40, 10:40–11:10, 11:10–11:40, 11:40–12:10, 12:10–12:50, 12:50–13:35, 13:35–14:40, 14:40–15:58 UT) and we evaluated [Fe XVIII] and Si XII line intensity in the CS over these intervals (for the Si XII line we also subtracted the quiet corona background). In each exposures group, emission in [Fe XVIII] line appears at a position roughly constant in time, while, adjacent to this feature, additional bright peaks show up, with variable intensities and spatial distribution. The spatial distribution of the [Fe XVIII] features observed is shown in Figure 2 (left panel), where the main structure is identified as the CS (solid line) and the adjacent intermittent features are represented by dotted lines. The identification of the bright [Fe XVIII] emission with the CS associated with the CME is supported by the correspondence between the P.A. of the CS in Figure 2 and the position of the LASCO bright "stem" below the CME bubble in Figure 1. We note that in Figure 2 (left panel) we reported the P.A. average

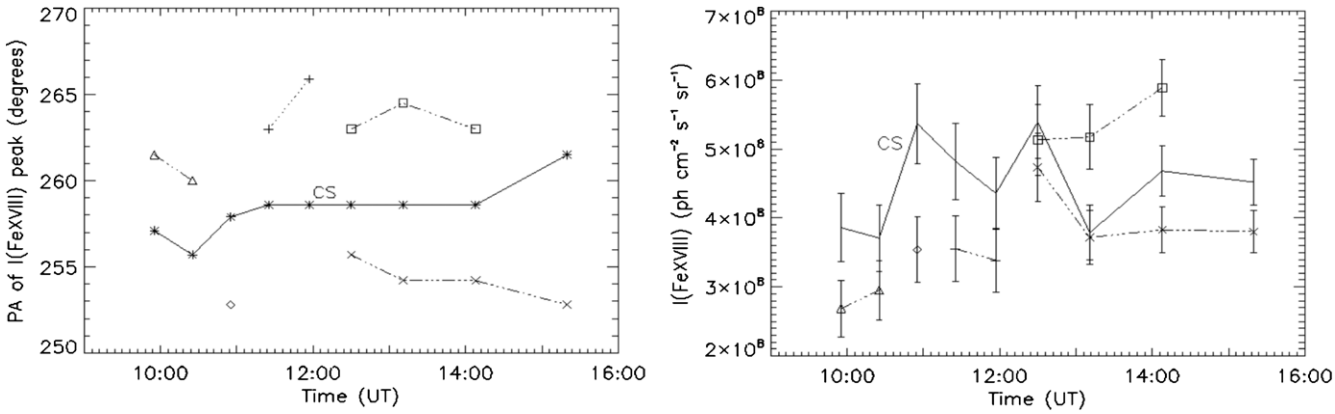

Figure 2. Spatial distribution (P.A., left panel) and [Fe XVIII] line intensity (in units ph cm^{-2} s^{-1} sr^{-1}, right panel) of the CS (solid line) and of the adjacent features (dotted lines) vs. time until the end of the observations. Symbols in the right panel identify corresponding features in the left panel.

value of the features observed in [Fe XVIII]: the solid line gives the average P.A. value of the CS, which has a width projected onto the plane of the sky between 5° and 7°, corresponding to $l = 1.5$–2.1×10^5 km, while adjacent structures (dotted lines) are thinner. Typical values for the CS width at $1.7R_\odot$, inferred by previous authors, are, e.g., $l = 6 \times 10^5$ km (Bemporad et al. 2006) and $l = 1.4 \times 10^5$ km (Ciaravella & Raymond 2008), in good agreement with the present measurement.

Figure 2 (right panel) shows the intensity versus time distribution of each feature observed in [Fe XVIII]. Two intensity enhancements in the main CS structure appear between 10:40–11:10 UT and 12:10–12:50 UT. Also transient enhancements of variable durations, with an intensity of the same order or slightly lower than that of the CS, appear on both sides of the CS.

3. PHYSICAL PARAMETERS OF THE TRANSIENT BRIGHTENINGS

In this section, we infer the values of electron temperature, electron density and mass in the observed transient brightenings, classifying them as blobs associated with the CME and CS inhomogeneities.

To this end, we derived the electron temperature (T_e) value from the intensity ratio of lines formed by collisional excitation, using the relation

$$\frac{I(X_a)}{I(Y_a)} = \frac{A_X}{A_Y}\frac{C(T)_{X_a}}{C(T)_{Y_a}}, \quad (1)$$

where X_a and Y_a are two generic ions of the elements X and Y respectively, A_X and A_Y are the abundances of the elements X and Y compared to that of the hydrogen, respectively, $C(T)$ is the contribution function depending on the collisional excitation coefficient and on the ionization balance. The emission of both ions has been assumed to originate from the same region.

Knowing the electron temperature, the emission measure, $\mathrm{EM} = \int_{\mathrm{LOS}} N_e^2\, dl$ (where N_e is the electron density and the integration is computed along the line of sight, LOS), can be evaluated from the expression of the collisionally excited intensity, I, of a coronal line, given by

$$I = \frac{1}{4\pi}\int_{\mathrm{LOS}} A_X\, C(T)\, N_e^2\, dl, \quad (2)$$

and the electron density can be derived, once a preselected L value has been assumed. Assuming blobs associated with the CME front to be spherical, L can be taken equal to their diameter.

Table 2
Physical Parameters of the Blobs Associated with the CME

Blob	log T_e	N_e (cm^{-3})	L (arcsec)	Mass (g)
1	6.08	6.0×10^7	168	3.2×10^{14}
2	5.25	1.1×10^7	126	5.9×10^{13}
3	5.24	2.5×10^7	210	5.3×10^{14}
4	5.21	9.0×10^7	126	4.8×10^{14}

3.1. Blobs Associated with the CME

Lines in the corona may form not only by collisional but also by radiative excitation, whenever the line emission from the solar disk is high enough. However, if the O VI 1031.9 to 1037.6 Å line ratio is around 2, we can safely assume that the O VI 1031.9 Å line forms only by collisional excitation (Noci et al. 1987). As to the C III line, it increases by a factor nearly 10^3 at the time the front and the blobs appear, so this line as well forms by collisional excitation only.

Hence, we used the ratio of O VI 1031.9 Å to C III 977.0 Å line intensity to derive the value of the electron temperature in the plasmoids listed in Table 1, assuming an abundance ratio $\frac{A_O}{A_C} = 2.0$ (Feldman et al. 1992) and the contribution functions from CHIANTI database (ver. 5.2) with the ionization balances from Mazzotta et al. (1998). We, then, measured the projected dimension, L, of each blob and used the observed O VI 1031.9 Å line intensity to infer its electron density and mass. The values of electron temperature, electron density, L, and mass obtained as described above are shown in Table 2 for blobs 1–4. Because blob 5 is detectable only in the C III line, we are unable to study its properties.

We note that the first blob is much hotter than the others, which show a temperature lower than the ambient corona and comparable with the temperature we inferred in the CME front (of about 2×10^5 K). The hot material may well be the result of the reconnection-heated plasma that enters the outer shell of the CME bubble through the upper tip of the CS, as predicted by Lin et al. (2004). Alternatively, it might have been produced together with a M3.9 flare, observed at the west limb by the Learmonth Observatory, at 08:41 UT at P.A. = 259°. This process would be analogous to that observed by Ohyama & Shibata (2008), who described the occurrence of a flare accompanied by hot and cold plasmoids. Blobs vary in density as well, although the assumption of a spherical symmetry may affect our estimates. Under this assumption, the mass is roughly the same for each blob.

3.2. CS Inhomogeneities

Figure 2, right panel, shows that [Fe XVIII] line intensity in the CS is not constant with time but shows enhancements of about 25% over its basic value. Using also the Si XII line intensity at the CS position, we derived the electron temperature and density of the CS. It turns out that at the times of the [Fe XVIII] intensity enhancements, the electron temperature shows insignificant changes with respect to its average value, while, assuming a constant CS thickness, the electron density increases by 10%–20%. These changes are too small to allow us to draw any conclusion about the process that originates the fluctuations.

The behavior of the [Fe XVIII] line sideways of the CS position seems more interesting. It is well known that the projected thickness of the CSs, as imaged by LASCO, or as inferred from the spatial extent of the [Fe XVIII] line emission in UVCS spectra, is much larger than expected from the theory. This observational result worsened the problem of identifying the nature of resistivity within the CSs, and led, e.g., Lin et al. (2007) to invoking a hyperresistivity as yet not fully understood (see, e.g., Strauss 1988). On the other hand, the CS may be thought as an ensemble of mini-structures, not detectable by present instrumentation, where the resistivity problem is alleviated. The filamentary nature of CSs has been predicted theoretically by Lee & Fu (1985) and Lee (1995) and confirmed by CLUSTER observations in the magnetotail (e.g., Slavin et al. 2003, 2005; Eastwood et al. 2005): plasmoids observed by CLUSTER well fit a scenario of multiple X-lines where reconnection takes place and produces plasmoids. Observations have also shown that one of the many X-lines, for so far unknown reasons, becomes dominant (Sharma et al. 2008).

Drawing upon the analogies between reconnection in the magnetosphere and in the solar atmosphere (Lin et al. 2008), we then suggest that the solid line in Figure 2 is the solar counterpart of the magnetospheric dominant X-line, while adjacent X-lines show up intermittently only at the time of plasmoid ejections. Temperatures and densities in these features have been derived from the ratio of Si XII to [Fe XVIII] line intensities. Because the Si XII to [Fe XVIII] emissivity ratio versus temperature curve has a concave shape with a minimum at $\log T = 6.9$, in the vicinity of this temperature two values correspond to a unique value of the line ratio. However, whatever choice is made, we can say that the electron temperature T_e in the regions of intermittent [Fe XVIII] brightening are $6.8 \leqslant \log T_e \leqslant 7.0$. Assuming $L = 8 \times 10^4$ km, which is consistent with Vršnak et al. (2009), we obtain that electron densities are $1 \times 10^7 \leqslant N_e \leqslant 2 \times 10^7$ cm^{-3}. These values are well compatible with other determinations of the physical parameters of CSs (e.g., Ko et al. 2003; Bemporad et al. 2006; Ciaravella & Raymond 2008).

The fluctuations in the dominant CS may originate from the passage of plasmoids. However, we seem to be able to identify them individually only in structures thinner than the main CS, where their emission contributes significantly to the LOS emission.

4. CONCLUSIONS

In previous sections, we discussed some unusual characteristics of transient brightenings associated with a CME, which appeared in lines from both cool and hot ions. Cool blobs, as described in the Section 1, have indeed already been observed with UVCS in the CS following a CME (Ciaravella & Raymond 2008). Here, we show that they may appear also in the main CME body, that is, in the CME bubble itself. Evidence for this comes both from UVCS spectra, where transient emission from blobs with a density higher by nearly a factor of 10 than in streamers (Gibson et al. 1999) have been detected, and from LASCO images (see Figure 1, right panel, where a few blobs are visible in the outer shell of the CME bubble). The average mass of cool blobs turns out to be about 5×10^{14} g, hence the typical CME mass of 10^{15}–10^{16} g may well be provided entirely by blobs. If such was the case, a CME would mostly consist of mini-CMEs, originating from the nearly simultaneous opening of field lines within a magnetic field line system. The identification of a hot plasmoid in the CME front may confirm the Lin et al. (2004) model prediction. According to these authors hot plasma originating in the reconnecting CS enters the outer shell of the CME bubble and contributes to its mass.

The interpretation of transient fluctuations in intensities of lines from hot ions is apparently more elusive. Here, we focused on the previously uninvestigated intermittent appearance of [Fe XVIII] 974.9 Å line brightenings, sideways of the CME-associated CS. We surmise that these brightenings, where the [Fe XVIII] line intensity is approximately equivalent to the CS brightness, are a manifestation of secondary X-line reconnection in a scenario analogous to the filamentation and multiple X-line reconnection previously suggested and recently observed in the Earth's magnetotail. Although we cannot claim this to be the unique interpretation of the data presented in this work, the consistency of our picture with the magnetospheric one leads us to list this as a further item in the analogies between solar and terrestrial reconnection.

The authors acknowledge support from ASI/INAF I/015/07/0. *SOHO* is a project of international collaboration between ESA and NASA. G.P. thanks ISSI (International Space Science Institute, Bern) for the hospitality provided to the members of the team on the Role of Current Sheets in Solar Eruptive Events where some of the ideas presented in this work have been discussed. This article has benefitted from constructive suggestions by the referee.

REFERENCES

Bárta, M., Karlický, M., & Žemlička, R. 2008, Sol. Phys., 253, 173
Bemporad, A., Poletto, G., Suess, S. T., Ko, Y.-K., Schwadron, N. A., Elliott, H. A., & Raymond, J. C. 2006, ApJ, 638, 1110
Carmichael, H. 1964, in Proc. of AAS-NASA Symp. on Physics of Solar Flares, ed. W. N. Hess (NASA-SP 50; Washington, DC: NASA Science and Technical Information Division), 451
Ciaravella, A., & Raymond, J. C. 2008, ApJ, 686, 1372
Ciaravella, A., Raymond, J. C., Li, J., Reiser, P., Gardner, L. D., Ko, Y.-K., & Fineschi, S. 2002, ApJ, 575, 1116
Eastwood, J. P., et al. 2005, Geophys. Res. Lett., 32, L11105
Feldman, U., Mandelbaum, P., Seely, J. F., Doschek, G. A., & Gursky, H. 1992, ApJS, 81, 387
Furth, H. P., Kileen, J., & Rosenbluth, M. N. 1963, Phys. Fluids, 6, 459
Gibson, S. E., Fludra, A., Bagenal, F., Biesecker, D., Zanna, G. D., & Bromage, B. 1999, J. Geophys. Res., 104, 9691
Hirayama, T. 1974, Sol. Phys., 34, 323
Hones, E. W., Jr. 1985, Aust. J. Phys., 38, 981
Hones, E. W., Jr., et al. 1984, Geophys. Res. Lett., 11, 5
Ko, K.-Y., Raymond, J. C., Lin, J., Lawrence, G., Li, J., & Fludra, A. 2003, ApJ, 594, 1068
Kopp, R. A., & Pneuman, G. W. 1976, Sol. Phys., 50, 85
Lee, L. C. 1995, in A Review of Magnetic Reconnection: MHD Models, Phys. Magnetopause (Washington, DC: American Geophysical Union), 139
Lee, L. C., & Fu, Z. F. 1985, Geophys. Res. Lett., 12, 105
Lin, J., Cranmer, S. R., & Farrugia, C. J. 2008, J. Geophys. Res., 113, A11107
Lin, J., & Forbes, T. G. 2000, J. Geophys. Res., 105, 2375

Lin, J., Ko, Y.-K., Sui, L., Raymond, J. C., Stenborg, G. A., Jiang, Y., Zhao, S., & Mancuso, S. 2005, ApJ, 622, 1251
Lin, J., Li, J., Forbes, T. G., Ko, Y.-K., Raymond, J. C., & Vourlidas, A. 2007, ApJ, 658, L123
Lin, J., Raymond, J. C., & van Ballegooijen, A. A. 2004, ApJ, 602, 422
Mazzotta, P., Mazzitelli, G., Colafrancesco, S., & Vittorio, N. 1998, A&AS, 133, 403
Noci, G., Kohl, J. L., & Withbroe, G. L. 1987, ApJ, 315, 706
Ohyama, M., & Shibata, K. 2008, PASJ, 60, 85
Priest, E. R., & Forbes, T. G. 2000, in Magnetic Reconnection: MHD Theory and Applications (New York: Cambridge Univ. Press)
Raymond, J. C., Ciaravella, A., Dobrzycka, D., Strachan, L., Ko, Y.-K., Uzzo, M., & Raouafi, N.-E. 2003, ApJ, 597, 1106
Riley, P., Lionello, R., Mikić, Z., Linker, J. A., Clark, E., Lin, J., & Ko, Y.-K. 2007, ApJ, 655, 591
Sharma, A. S., et al. 2008, Ann. Geophys., 26, 955
Slavin, J. A., et al. 1984, Geophys. Res. Lett., 11, 657
Slavin, J. A., et al. 2003, Geophys. Res. Lett., 30, 2208
Slavin, J. A., et al. 2005, J. Geophys. Res., 110, A06207
Strauss, H. R. 1988, ApJ, 326, 412
Sturrock, P. A. 1966, Nature, 211, 695
Vršnak, B., et al. 2009, A&A, in press